
# HYDROGEN STORAGE SYSTEM DESIGN: CASE STUDIES FOR AIRBORNE APPLICATION

Filippo Mazzoni[1,*], Grazia Accardo[2], Roberta Biga[2], Eugenio Brusa[1], Cristiana Delprete[1], Camilo Andrés Manrique-Escobar[2] & Valeria Vercella[2]

[1]Department of Mechanical and Aerospace Engineering, Politecnico di Torino, Corso Duca degli Abruzzi 24, Torino, 10129, Italy
[2]Leonardo Innovation Labs & Intellectual Property, Leonardo S.p.A., Corso Francia 426, Torino, 10146, Italy

## Abstract

Hydrogen represents one of the most promising alternatives to fossil fuels in reaching net-zero emissions targets. In addition, the high energetic content of hydrogen, together with the development of innovative technologies, can be exploited to design aircraft with improved performance. In the present study, the $H_2$ vessel parametric model is described, validated, and applied to two case studies: a regional aircraft (ATR) and an Unmanned Aerial Vehicle (UAV). Results show that increases in the tank gravimetric efficiency up to 30.30% can be achieved, thus leading to relevant weight saving of 207 kg, for the ATR and to a flight endurance of 73.33 hour for the UAV. Moreover, the outputs of the analysis demonstrate, from a preliminary design perspective, that the technology targets set by the main institutional organizations can be accomplished if efforts are invested in developing innovative technologies.

**Keywords:** Parametric design, Hydrogen storage, Aviation, Regional aircraft, UAV

## 1. Introduction

The carbon footprint reduction has become a critical issue to be faced immediately to decrease the negative environmental impact before crossing the point of no return. Referring to the mobility sector, this coincides with reducing the polluting exhaust gases emitted, which translates into substituting fossil fuels. As pursued by the Clean Sky program ([1]), one of the most promising solutions to reach zero-emission targets can be hydrogen. The main reasons behind that are the large availability of hydrogen, its capability of satisfying requirements coming from different industrial needs and, focusing on the mobility sector, its high specific energy content that can be exploited through zero-emissions powertrains when fuel-cells are used.

Hydrogen can be stored on-board in different forms that are classifiable in two main categories: physical-based and material-based methods. The former includes systems storing hydrogen in liquid ($LH_2$), cryo-compressed ($CcH_2$), and compressed ($CH_2$) forms. $CcH_2$ can be seen as a method halfway between the other two, where $H_2$ is at high pressures and cryogenic temperatures. These methods are at a higher technology readiness level (TRL) if compared to the materials-based methods that, instead, exploit the capability of certain materials, such as metal hydrides, to chemically bond to hydrogen molecules [2].

The amount of studies in literature focusing on the use of hydrogen in aviation is increasing in time and encompasses different topics and applications such as hydrogen powered aircraft [3], boil-off management [4], liquid hydrogen fuel systems integration in unmanned aerial vehicles [5], as well as mission characteristics ([6], [4]) and studies on hydrogen-fueled regional airliners [7].

Literature analysis highlighted the need for quantitative results related to key aspects of hydrogen storage systems, such as the system mass, volume, shape, and materials, to be at a proper level of detail. Thus, a sizing model has been structured to be adopted from the initial design phases to understand the influence of various design choices from geometrical, mechanical, and thermal perspectives. The implementation of the model will drive further design steps by defining the most suitable pathways to optimize the system properties. In the present work, the model, described in Section 2.and shown in Figure 1, will be applied to two case studies of two aircraft belonging to different categories. The main issues faced during design will be highlighted together with the main aspects deriving from the applications selected.

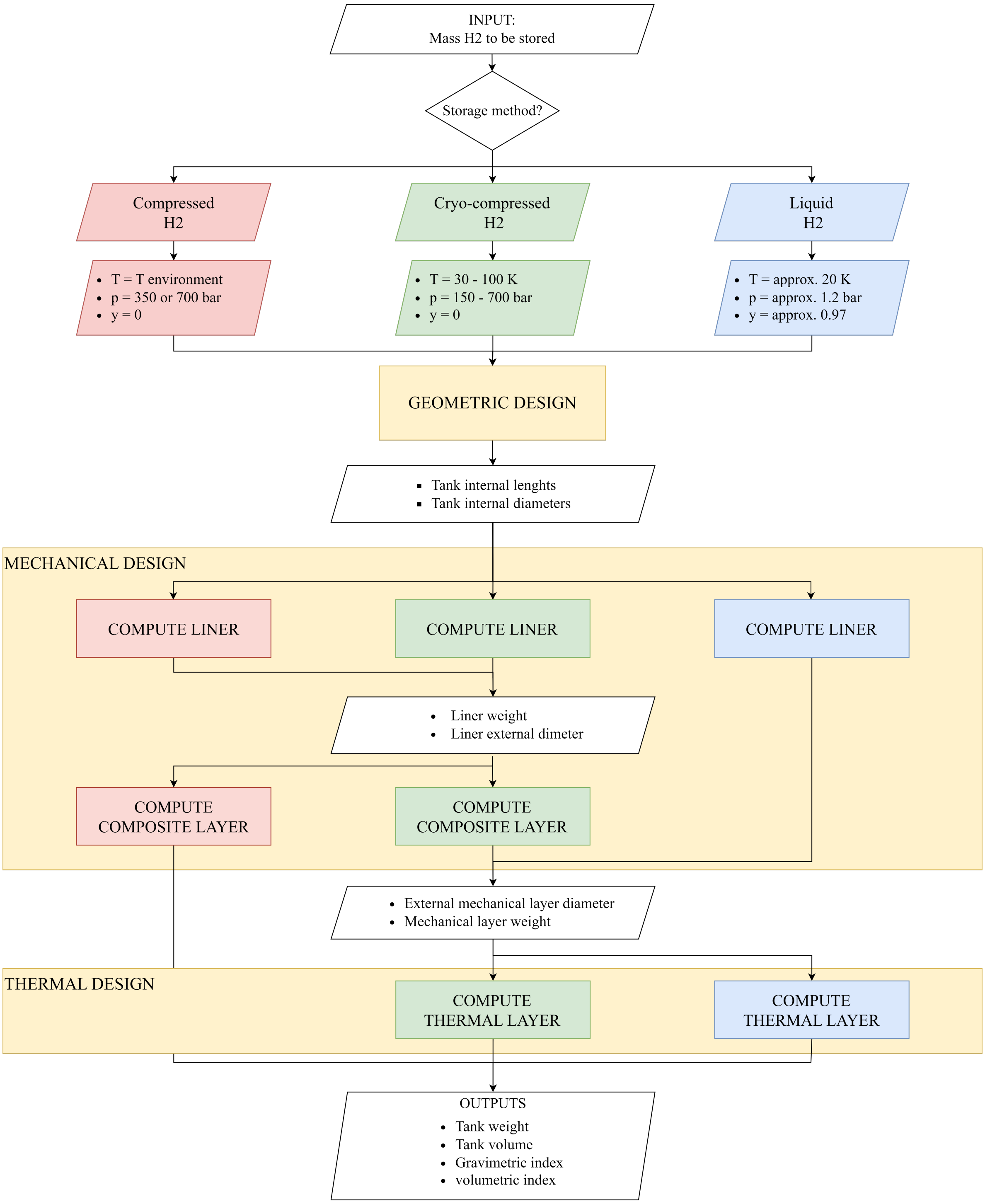


Figure 1 – Parametric sizing model workflow for preliminary design of hydrogen tank.

## 2. Methodology

The preliminary design model (Figure. 1) takes the mass of hydrogen to be stored as input and gives the tank dimensions and weight as outputs. In addition, it also provides the gravimetric index that will be used to identify the optimal trade-off among different solutions. The sizing tool explores the three physical-based methods of storing hydrogen ($LH_2$, $CcH_2$, and $CH_2$), even if, in the following analysis, greater attention is devoted to the $LH_2$ storage, considered the most present in many analyses. The design is performed in three subsequent steps, corresponding to three Python scripts: geometric, mechanical, and thermal design, detailed in the subsequent sections. Moreover, being the model parametric, comparisons among different solutions or changes in the design parameters are very easy to implement.

### 2.1 Geometric design

The geometric design module receives, as external input, the hydrogen mass and computes the vessel's internal volume for each storage method, corresponding to different thermodynamic conditions. Then, the internal dimensions are calculated for a given tank shape, consisting of a vessel with a cylindrical central body and, alternatively, hemispherical or semi-elliptical domes (as shown in Figure 2). The design parameter to be set as input is $\beta$, i.e., the ratio between tank diameter ($D$) and length ($L$), as reported in Eq. 1.

$$\beta = D/L \qquad (-) \tag{1}$$

As shown in Figure 2, for $\beta$ tending to zero the tank has an elongated shape while, for $\beta$ tending to one, it is shorter and stocky. It is worth mentioning that, in the particular case of $\beta = 1$, the tank shape corresponds to a sphere. Spherical geometries hold the lowest Area-to-Volume Ratio (AVR) and will be used as a benchmark in further analyses. For fixed amounts of hydrogen stored, lower AVRs correspond to smaller surfaces that translate into lighter tanks and lower amounts of heat exchanged through tank walls. Usually, the vessel shape is constrained by the integration inside the aircraft structure and by manufacturing limitations [3]. A typical value of $\beta$ is $0.66$, consisting of a diameter that is two-thirds of the tank length, and it will be the parameter used if not differently specified.

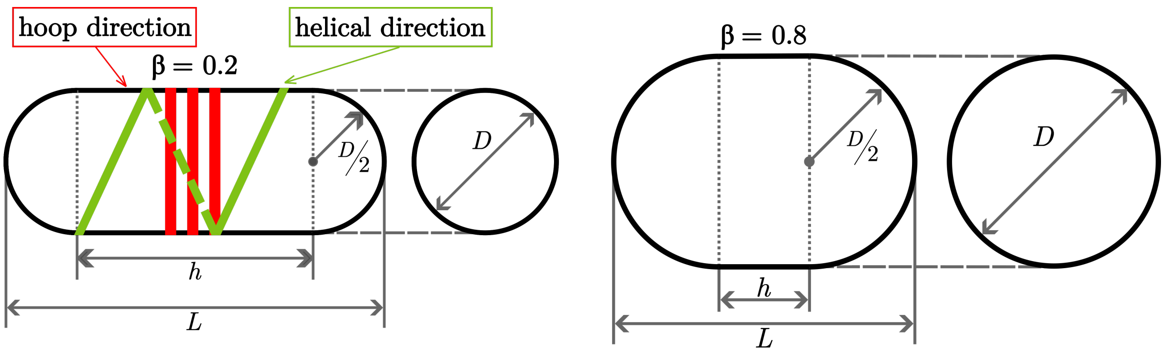


Figure 2 – Tank shape for varying diameter-over-length ratio $\beta = 0.2$: $\beta = 0.2$ on the left and $\beta = 0.8$ on the right; qualitative representation of the fiber hoop (in red) and helical (in green) directions in the left picture.

### 2.2 Mechanical design

The innermost layer is meant to bear stresses generated by internal pressures. In addition, being directly in contact with hydrogen, it should also avoid $H_2$ permeation and resist embrittlement phenomena. Indeed, due to the very small dimension of its molecules, hydrogen is able to permeate through certain materials ($H_2$ permeation) and, after long exposures, it can deteriorate the structural properties of materials and, in the worst scenarios, it can even be the cause of brittle fractures at relatively low applied stresses ($H_2$ embrittlement) [3]. So, concerning the use of metallic materials, the well-assessed properties of aluminum alloy Al 6061, both at ambient and cryogenic temperatures, assure an excellent resistance to permeation and embrittlement, and it will be implemented both in the case of $CH_2$ and $LH_2$ [8]. Instead, a High Density Polyethylene (HDPE) polymeric material has been implemented in the analysis of $CH_2$ vessels only [9]. The adoption of polymeric materials at

cryogenic temperatures should be further investigated, especially considering their ductile-to-brittle transition, but this objective goes beyond the scope of the present study.
The thickness of the mechanical layer has been computed according to the following formulas.

$$S_{F,burst} = \frac{p_b}{p_s} \qquad (-) \tag{2}$$

$$t_{\text{tot,layer,hoop}} = \frac{p_b \cdot R_C}{\sigma_{cr,fib} \cdot V_f}\left[1 - \frac{1}{2}\tan^2(\alpha_c)\right] \qquad (m) \tag{3}$$

$$t_{\text{tot,layer,helical}} = \frac{p_b \cdot R_C}{2 \cdot SR \cdot \sigma_{cr,fib} \cdot V_f \cdot \cos^2(\alpha_c)} \qquad (m) \tag{4}$$

$$t_{\text{wall}} = \text{Max}\left(\frac{1.5PR}{Sy}, \frac{2.25PR}{Su}\right) \tag{5}$$

Eq. 2, 3, and 4 are derived from standards ISO 11439 (2000) and ASME Sec. X (2004) ([10], [11]) and are used for the preliminary sizing of composite fiber vessels to store compressed and cryo-compressed hydrogen. The burst safety factor (Eq. 2), derived from ASME Sec. X (2004), is defined as the ratio between burst pressure ($p_b$: maximum pressure level before rupture (MPa)) and service pressure ($p_s$: internal tank pressure during normal operating conditions (MPa)). The value of $p_b$, derived from Eq. 2, is then used in Eq. 3 and 4 to compute the thicknesses of the composite material along the hoop ($t_{\text{tot,layer,hoop}}$ (m)) and the helical ($t_{\text{tot,layer,helical}}$ (m)) directions (represented in Figure 2). The parameters in Eq. 3 and 4 are: $R_C$ (m) the cylinder radius, $\sigma_{cr,fib}$ (MPa) the fiber ultimate strength, $V_f$ (-) the fiber-to-composite volume fraction, and $\alpha_c$(rad) is the cylinder fiber angle (angle between fiber and longitudinal cylinder directions).

The use of composite materials is particularly suitable for compressed $H_2$, both at ambient and cryogenic temperatures. Indeed, when composite material is present, it is assumed that the internal liner does not carry any load and is only meant to avoid hydrogen permeation and resist hydrogen embrittlement. According to the above mentioned Figure 1, it can also be noted that there is no composite layer computation for the $LH_2$. This is due to the low service pressures at which $H_2$ is stored in liquid form, avoiding the need to use composite materials. The choice of storing $LH_2$ at low pressure levels finds an explanation in Figure 3: $LH_2$ density decreases with increasing pressure, and since a higher density means higher $LH_2$ mass stored for a fixed volume, the $p_s$ is kept as low as possible. Conversely, a $p_s$ below the external environmental pressure is strongly not recommended to avoid ambient air infiltration in case of tank damage [3]. So, a $p_s$ slightly higher than the external pressure is mostly desired. In conclusion, in $LH_2$ vessels, the service pressures are so low that the use of composite materials is not worth it.The mechanical layer reduces to the metallic liner itself, which must be designed to bear mechanical loads as the only structural component and is also meant to avoid $H_2$ permeation and embrittlement. Hence, the tank wall thickness ($t_{\text{wall}}$) in the case of $LH_2$ vessels is computed with Eq. 5, derived from ASME VIII [12], where $P$ is the maximum internal pressure, $R$ is the inner radius, $Sy$ the yield strength, and $Su$ the ultimate tensile strength of the material. In addition, in consideration of the fact that $t_{\text{wall}}$ can be computed starting from $Su$ or $Sy$, the maximum between the two values of the thickness has been selected (Eq. 5).

To increase the load-bearing capacity of Type I vessels, the weight calculation can be adjusted by a correction factor, expressed as a percentage of the mechanical layer weight, to account for extra geometric features that enhance threads and joints. In section 3this parameter has not been adopted considering the wide spectrum of results found in literature while, in section 5.a $10\%$ correction factor has been applied.

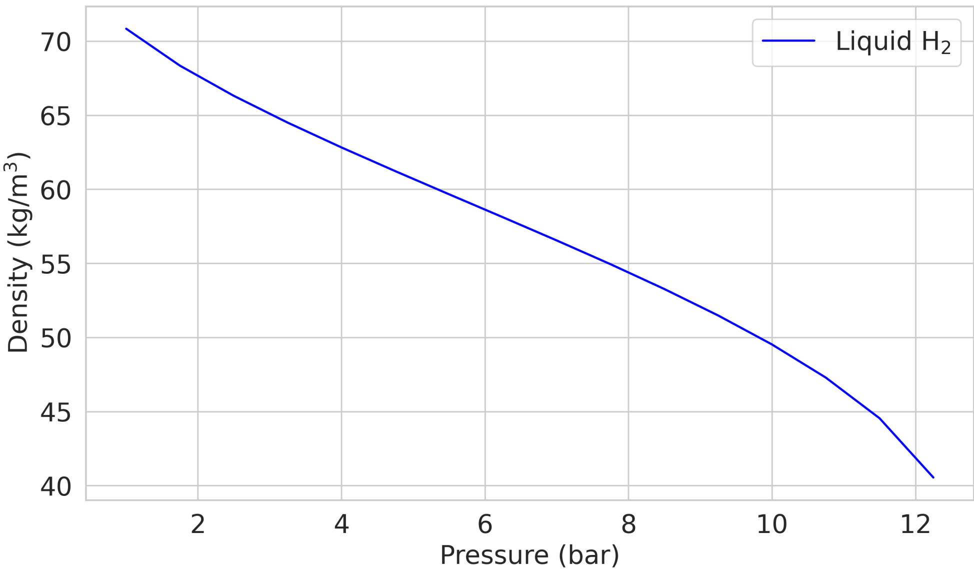


Figure 3 – Liquid hydrogen density as a function of pressure.

## 2.3 Thermal design

At ambient pressure, liquid hydrogen evaporates at -252.88℃. Keeping the $H_2$ in liquid form for extended and properly managing the rate at which it evaporates (boil-off rate) represent some of the hardest technical challenges in $LH_2$ storage [3]. In the present study, this is the starting point for the thermal design performed through Eq. 6 and Eq.7. It follows further that the choice of proper insulation materials becomes crucial for the whole system design. The present analysis proposes the investigation of $LH_2$ vessel sizing implementing four insulating materials (Table 1), intending to compare the outcomes with the use of two well-assessed materials, namely rohacell and polyurethane, and two more innovative and performing solutions: Multi-Layer Insulation Mylar/Dacron (MLI MD) and Aerogel/Glass Fiber, both working at pressures lower than the environmental (referred to as "low pressure" in Table 1).

$$Q_{in} = \frac{T_{ext,env} - T_{inner\ surface}}{R_{total}} \qquad (W) \tag{6}$$

$$BOR = \frac{Q_{bor} \cdot 24 \cdot 3600 \cdot 10}{V_{LH_2} \cdot \rho_{LH_2} \cdot H_{vap} \cdot 100} \qquad (\%/hour) \tag{7}$$

The correlation between thermal layer thickness and boil-off gases, expressed as boil-off rate (BOR) $(\%/\mathrm{h})$, is set through Eq. 6 and 7. In Eq. 6, $Q_{in}$ (W) is the heat entering the tank, $T_{ext,env}$ (K) the temperature of the external environment (computed as ISO $+ 35\,^\circ\mathrm{C} = 50\,^\circ\mathrm{C}$), and $T_{int,surface}$ (K) is the temperature of the internal tank surface. $R_{total}$ is the sum of the thermal resistances subdivided into external natural convection and internal conductive resistance. In Eq. 7, $V_{LH_2}$ $(\mathrm{m}^3)$, $\rho_{LH_2}$ $(\mathrm{kg/m}^3)$ and $H_{\text{vap}}$ $(\mathrm{J/kg})$ are hydrogen volume, density and latent heat of vaporization [13].

As shown in Figure 4, the various thermal resistances are modeled using the electric resistance circuit analogy [13]. However, the heat leakages due to the conduction through the tank supports and pipes can hardly be quantified at a preliminary design level. Thus, a correction factor has been introduced to increase the heat entering through the tank by 30% [14].

To calculate a tank's thermal conduction and convection resistance, it is necessary to know the radii of the various layers and their thicknesses. However, determining these values is part of the problem to be solved. To address this issue, an optimization algorithm has been developed to determine the optimal thickness value. This value ensures that the heat power entering the tank ($Q_{in}$) stays below a specified boil-off rate value ($Q_{bor}$) while minimizing the tank's weight.

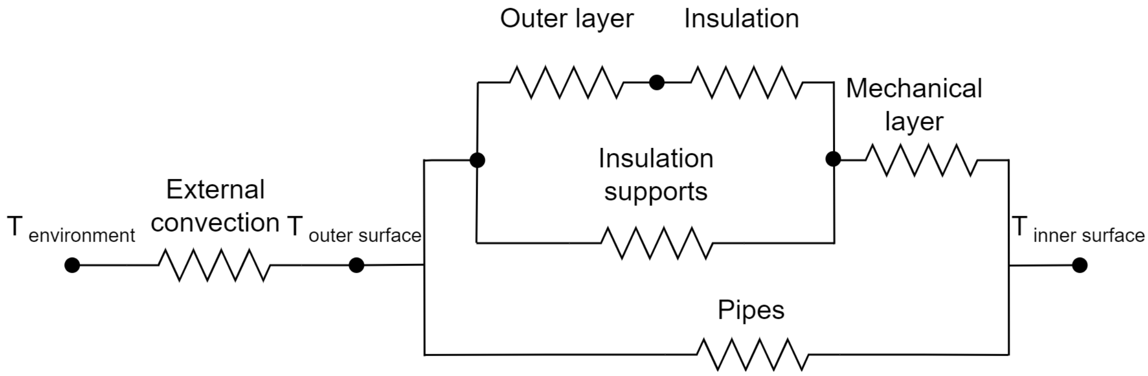


Figure 4 – Tank wall thermal resistances equivalent circuit.

The outputs of thermal design are the thickness and weight of the insulating layer that, added to the outputs from previous steps, result in the total tank weight and volume.

Table 1 – Insulation materials properties.

| Material | Density $(kg/m^3)$ | Thermal conductivity $(W/mK)$ | $\rho \cdot k$ | Bib. Ref. |
|---|---|---|---|---|
| Rohacell® 41S | 51.1 | 0.0311 | 1.589 | [15] |
| Polyurethane - rigid, open cell | 40 | 0.0245 | 0.980 | [16] |
| Aerogel/Glass Fiber low pressure | 125 | 0.0006 | 0.075 | [15] |
| MLI Mylar/Dacron low pressure | 40 | 0.00007 | 0.0028 | [15] |

## 3. Model validation

A relevant part of the work presented here was dedicated to an extensive literature review aimed to gather a considerable amount of data to validate the preliminary design model described in the previous sections. Table 2 presents a series of gravimetric index values for the three physical storage methods: $CH_2$, $CcH_2$, and $LH_2$. Most of the retrieved data pertains to $CH_2$ and $LH_2$, while only a few values have been found for the less-investigated case of $CcH_2$, which is the least researched among the various publications.

The gravimetric index range for liquid hydrogen vessels is very wide, ranging from 7.5% to 90%. This is because this technology has a broad range of applications. Studies related to LH2 vessels have been applied to different aircraft types, from small Unmanned Aerial Vehicles (UAVs) to general aviation, regional, and long-haul airliners. Typically, higher gravimetric indexes are required for larger tank capacities.

Compressed hydrogen storage is the most mature technology of the three. It is less efficient but much easier and cheaper to implement and is usually limited to a few kilograms of storage capacity. $CH_2$ vessels are classified into five categories. The first two are Type I, fully made of metal, and Type II, made of metal with a limited amount of composite material in the central part. These two are not very interesting to the aviation sector because they are heavy.

Type III is made of a metal liner wrapped in composite material, while Type IV is the same as Type III, except the liner is made of polymeric material. Type V is liner-less. Type III and IV are commercially available for hydrogen storage. They have an operating pressure of 350 or 700 bar and usually hold a gravimetric index below 10%.

More innovative prototypes have been found in the literature that overcome these values by a few percentage points, as shown in Table 2. Type V liner-less pressure vessels are also available, although the direct interaction between hydrogen and composite material needs to be better understood, especially in the long-term effects.

Few values have been found for cryo-compressed $H_2$ vessels. For this case, validation has not

Table 2 – Gravimetric index literature values for parametric model validation.

| Storage type | Range (%) | Gravimetric index (%) | Notes | Bib. Ref. |
|---|---|---|---|---|
| $LH_2$ | **7.5 - 90** | 70.9 | Regional aircraft - Polyurethane insulation | [7] |
| | | 68.6 | Regional aircraft - Rohacell insulation | [7] |
| | | 67.5 | Regional aircraft - MLI insulation | [7] |
| | | 7.5 | Automotive applications | [2] |
| | | 10 | 20 K - 1,5 bar - Aviation | [17] |
| | | 30-90 | Aviation | [18] |
| | | 40 - 80 | Aviation | [15] |
| | | 30 | Regional aircraft | [9] |
| | | 35 | Short range aircraft | [9] |
| | | 65 - 70 | Long-range aircraft | [9] |
| | | 26 - 34 | 100 - 500 kg $H_2$ storage capacity | [9] |
| $CcH_2$ | **7 - 28** | 7 - 10 | 350 - 700 bar, 66.15 - 78.15 K - Aviation | [17] |
| | | 5 - 6 | 350 - 700 bar, 40.15 - 80.15 K - Aviation | [17] |
| | | 28 | 50 - 700 bar, 25 - 110 K - Aviation | [15] |
| $CH_2$ | **1 - 15** | 6.7 | 350 bar - Automotive applications | [2] |
| | | 6 | 350 bar - Automotive applications | [2] |
| | | 5.7 | 20℃, 700 bar - Aviation | [17] |
| | | 4 | Composite with metal liner - Aviation | [18] |
| | | 5 | Composite with polymer liner - Aviation | [18] |
| | | 6 | Linerless composite - Aviation | [18] |
| | | 1-15 | 350 bar - Aviation | [18] |
| | | 1-15 | 700 bar - Aviation | [18] |
| | | 5-10 | Aviation | [15] |
| | | up to 6 | Commercial vessel | [9] |
| | | up to 13 | Protoype vessel - Flight-tested | [9] |
| | | 10 - 15 | 100 - 300 kg $H_2$ storage capacity | [9] |

been performed due to the difficulties in testing and characterizing materials and systems under the combined effect of high pressure and cryogenic temperatures. However, cryo-$H_2$ in gaseous form holds higher densities than $LH_2$ for wide pressure-temperature intervals, and this, together with other advantages, could make it more attractive in the upcoming years.

The model validation is performed by comparing the literature data (Table 2) with outputs from the model reported in Figure 6 and Figure 5. Figure 5 shows the values of the gravimetric index for increasing vessel storage capacity. For the sake of completeness, it must be specified that no corrections factors have been applied to derive the outputs in the present section (Figures 5 and 6), neither for the mechanical (see Sec. 2.3) nor for the thermal design (see Sec. 2.2). A further validation of the results obtained taking into account the correction factors can be done looking at the results shown in the case studies (Sec. 5). However, in both cases, a good agreement between the results of the parametric model (Figures 5 and 6) and the data retrieved from the literature (Table 2) has been ascertained. The gravimetric index increases for increasing values of the $H_2$ mass stored and is bounded inside a range that approximately spreads from 10% to 70%.
Comparing the data related to the $CH_2$ from Table 2 and that computed with the model (Fig. 6), it can be seen that the values comprised by the curves are also in this case in good agreement with the tabular data. Indeed, the computed gravimetric index (Figure 6) falls within a range of values between 4.75% and 6.5%. In this case, the two curves characterizing an inner pressure of 350 bar (green and red in Figure 6) are both above those of 700 bar (red and orange in Figure 6), pointing out that if a higher gravimetric index is of primary importance, the choice of the tank operating pressure holds greater influence on the performance concerning the choice of the tank type (Type III or Type IV). All four curves describe a steep increase up to a storage capacity of 20 kg, which is more pronounced for the Type III tank at 350 bar, after which the trends tend to constant values of the gravimetric index. These results are coherent with those collected from the literature. Indeed, pressure vessels at 350 bar typically hold higher gravimetric indexes and lower volumetric efficiencies compared to those operating at 700 bar.

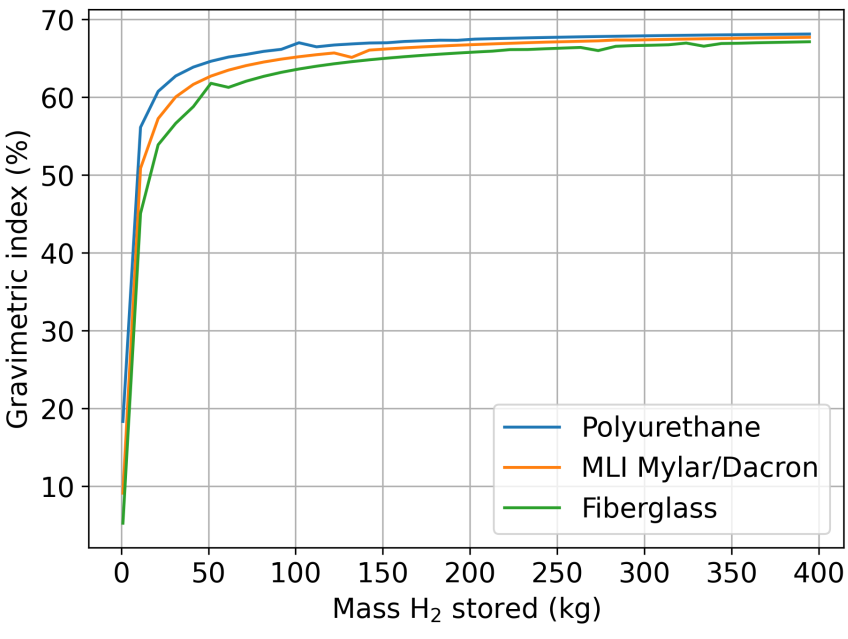


Figure 5 – Gravimetric index as a function of the $H_2$ mass stored inside the tank for liquid $H_2$ for three insulation materials (no correction factors applied, see Sec. 2).

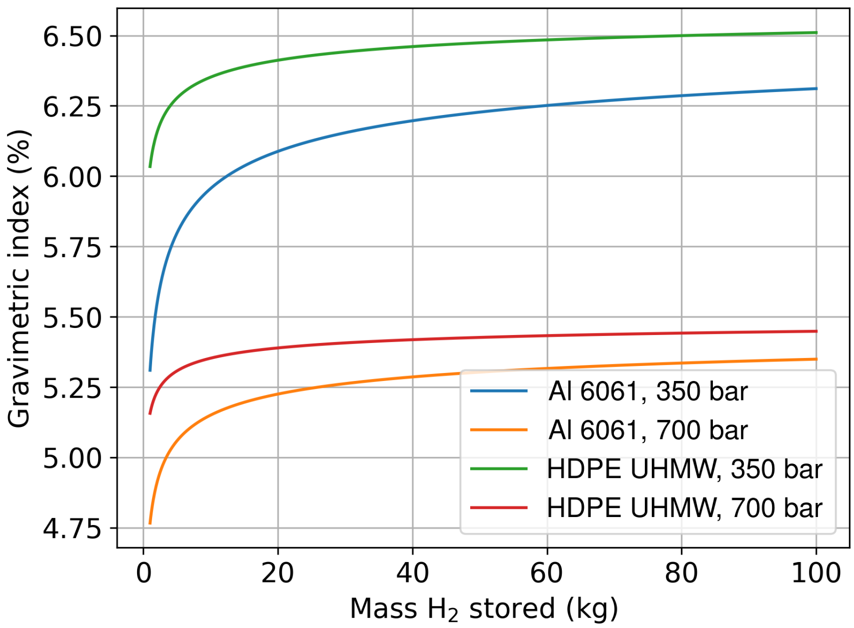


Figure 6 – Type III (Aluminum alloy Al 6061-O liner) and Type IV (High Density Polyurethane Ultra-High Molecular Weight HDPE UHMV polymeric liner) $CH_2$ tank gravimetric index for varying mass of $H_2$ stored for a fixed ratio of the tank diameter over length: $\beta = 0.66$.

## 4. Technological targets

The goal of achieving zero-emission aviation is a long-term endeavour, with major institutions aiming for a net-zero emission target by 2050 [19][20]. This may seem far, but it's significant to consider that aviation programs can last some decades. Additionally, achieving this goal requires substantial innovation across a wide range of applications, from airport infrastructure to aircraft powertrains.

Different roadmaps are drawn to define the intermediate steps to reach net zero in 2050. Usually, these twenty-five years are covered by three main phases. From 2025 to 2030, the first flight demonstrations and certifications are expected. Both the prototypes already manufactured and those under design result from retrofitting activities applied to regional and sub-regional demonstrators. From 2030 to 2040, the increased knowledge and technologies available in the market will allow an overall optimization at the system level. Narrow-body and regional airliners holding higher performance are expected from aircraft manufacturers such as Embraer ([21]), with a regional and a sub-regional turboprops powered by fuel-cells, and Airbus ([22]), delivering several concepts in the context of the ZEROe project. It has been foreseen that the demand for hydrogen supply from the aviation sector will be low up to 2040. In the final decade, from 2040 to 2050, hydrogen-powered aircraft fleets will be introduced together with long-haul airliners [15].

The road-maps traced provide values for many technology indicators describing the emissions reduction and the technological maturity of the main systems composing hybrid-electric aircraft architectures. Focusing on the hydrogen storage system, the future targets are based on the gravimetric index. The Clean Aviation Joint Undertaking in the Strategic Research and Innovation Agenda fixed its values for 2020 and 2024 at 12% and 16%, respectively. A value of 35% is is set for the 2030[23]. FlyZero published a road-map where the technology indicators are expressed separately for regional, narrow-body, and midsize airliners. Two values of the gravimetric index are distinguished for the aft tanks 1 and 2 (two tanks installed at different points of the aircraft fuselage) for the years 2026, 2027 and 2050. Taking into account the maximum between each couple of values, which only differ for a few percentage points, the target gravimetric index results to be 57% for 2026 and 75% for both 2030 and 2050 [24]. Other studies state that a gravimetric density of 50% ([17]) or 70% ([15]) is achievable by 2035.

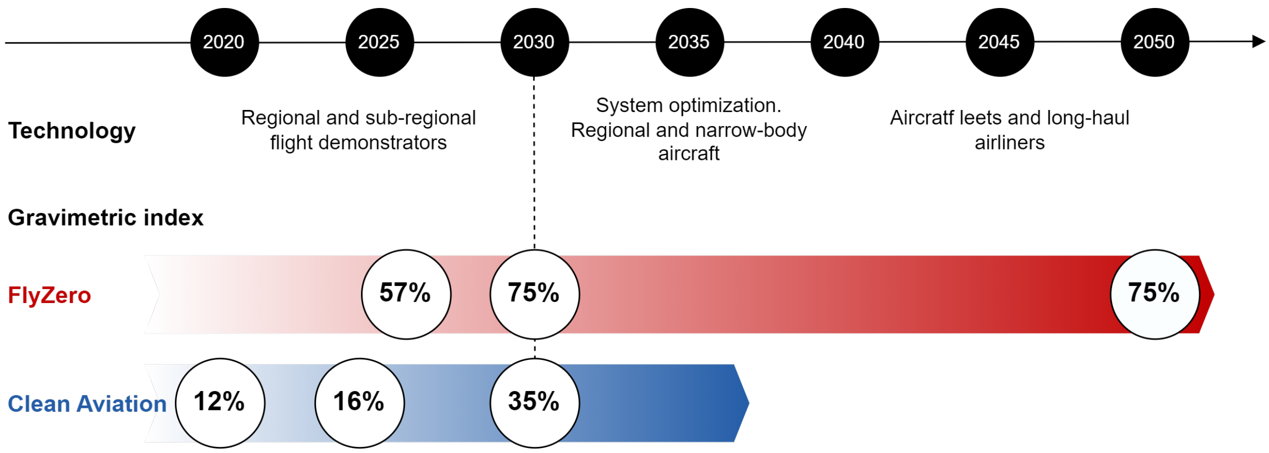


Figure 7 – Future technology and gravimetric index projections (elaborated from the Aerospace Technology Institute Flyzero project report [24]) and the Clean Aviation Strategic Research and Innovation Agenda [23]
.

## 5. Case studies

In the following sections, the previously described and validated model is applied to investigate two case studies. The first one involves the design exploration of a regional hybrid-electric aircraft considering different future scenarios [25]. The second use case describes the design of a $LH_2$ vessel to be integrated with a Proton Exchange Membrane Fuel-Cell (PEM FC) to power a small UAV [26].

In the first use case, Marciello et al. propose three scenarios: one related to the medium-term, where the aircraft is powered with a PEM fuel cell and a battery and the hydrogen is stored in gaseous form, and two long-term scenarios, where liquid hydrogen is used and converted into electricity using a PEM fuel cell, in one case, and a SOFC fuel cell in the other case [25]. The present study analyses the storage system to reduce the hydrogen tank weight and optimize the gravimetric index.

In the second use case, Adam et al. designed a liquid hydrogen vessel for a UAV to obtain a long endurance. Useful data related to the tank geometry, the weight of the thermal and mechanical shells and accessories, the overall system weight, and the fuel consumption have been extrapolated and used as a starting point for the investigation proposed here. The parametric model has been adopted to explore the impact of other solutions to increase UAV endurance further.

So, the model inputs have been set up for both use cases to satisfy the requirements extrapolated from the two studies, and the differences with the literature references have been highlighted. In the case of the regional airliner, the main advantages are shown in terms of weight savings, while for the UAV, the main findings have been quantified and translated into an increase in flight endurance.

### 5.1 Regional aircraft

A case study for the application of the tank parametric model has been selected from the literature. The study, developed by Marciello et al. [25], focuses on designing a 50-passenger regional aircraft with the ATR 42-600 as the baseline reference. The study explores different hybridization strategies using internal combustion engines, batteries, and fuel-cell systems. It offers projections for three future scenarios: short-term (2025-2035), medium-term (2035-2045), and long-term (2045-2050+). Although the authors' study covers all the aircraft's main systems, the present study focuses on the hydrogen storage system. The authors have chosen the most relevant data related to the hydrogen storage system from the information provided by Marciello et al. to analyze it in-depth.

As shown in Table 3, the storage system implemented in the mid-term scenario is based on compressed gaseous vessels, while that referred to the long-term scenario is based on cryogenic liquid hydrogen vessels. In the present study, the results referring to the mid-term scenario ($CH_2$) are reported in Table 4, while those obtained investigating the two solutions for the long-term scenarios

($LH_2$) are reported in Figure 8 and Figure 9, for the optimized gravimetric indexes and total system weights, respectively.
In addition, it can be noted that a gravimetric index of around 40% has been estimated in the long-term scenario, and that can be considered aligned with the forecast provided by Clean Aviation (Fig. 7).

Table 3 – ATR reference data from [25]

| Scenario | Storage type | Technology | Tanks number | Total Tanks weight (kg) | Total H2 mass (kg) | Gravimetric index (%) |
|---|---|---|---|---|---|---|
| Medium-term (2035-2045) | CH2 | PEMFC + Battery | 4 | 2685.6 | 390.7 | 10-13 |
| Long-term (2045-2050+) | LH2 | SOFC + Battery | 4 | 410.2 | 281.8 | 40-41 |
| | | PEMFC + Battery | 4 | 529.3 | 361.4 | |

Focusing on pressurized tanks, a gravimetric index of 12.7% has been estimated (Table 3). Keeping this value as a reference, different solutions have been proposed in the present analysis (Table 4). The various options include cylindrical body vessels with hemispherical and semi-elliptical domes, two different storage pressures of 350 bar and 700 bar, two different liners made of aluminum alloy Al 6061-O and Ultra-High Molecular Weight High-Density Polyethylene polymeric material (HDPE UHMW), commonly referred as Type-III and Type-IV vessels. A third Liner-less option has been added for comparison, usually called Type-V vessel, even though a proper investigation and selection of materials should be conducted considering this technology's lower maturity level.

Looking at Table 4, it can be seen that the gravimetric index is lower than that provided by the literature (Table 3) in all the cases. These discrepancies can be traced back to the formulas implemented to compute the tank wall thickness. Indeed, Marciello et al. [25] provide a future projection of the gravimetric index value (mid-term scenario in Table 3), while the authors here referred to what can be seen as a present scenario, relying on formulas from standards and materials commercially available (Sec. 2).

General conclusions can be drawn based on the results computed in this study for $CH_2$ storage (Table 4). Hemispherical dome shapes and storage pressures of 350 bar always provide higher gravimetric indexes. Concerning the liner, lower material densities hold higher gravimetric indexes, and no liner is the best option, keeping all the other characteristics unchanged.

Moving to the long-term scenario (Table 3), the total amount of hydrogen is stored in four equal cryogenic $LH_2$ tanks that are modeled considering 5% boil-off ratio of the hydrogen and perlite-vacuum insulation. The vessels hold gravimetric index values for both SOFC and PEMFC between 40% and 41% [25]. The study here presented starts from the same initial requirements of hydrogen mass to be stored in each of the four tanks, that are 70.45 kg and 90.35 kg for the cases of SOFC and PEMFC (Table 3), respectively, and performs an optimization aiming at improving tank performance. The insulation materials selected are four: polyurethane and Rohacell, exhibiting poorer insulating characteristics but higher reliability; Aerogel and Multi-Layer Insulation Dacron/Mylar (MLI MD), both used under a certain degree of vacuum, showing higher performance but considered to hold lower reliability (Table 1). The results are reported in terms of the percentage increase of the gravimetric index for each single tank (Figure 8) and the total storage system weight difference with respect to the reference cases (Figure 9).

After analyzing Figure 8, it can be concluded that higher tank capacities result in better improvements. The most efficient solution involves MLI MD, with a gravimetric index of 52.9% and 51.7% for the two $H_2$ masses in the legend. For the tank capacity of 70.45 kg (blue bars in Figure 8), the

Table 4 – Tank empty weights and gravimetric indexes referred to the medium-term scenario (Compressed $H_2$ tank storing a mass of hydrogen of 97.7 kg) with a diameter over length ratio $\beta = 0.66$.

| Caps geometry | Inner pressure | Liner material | Tank empty weigth (kg) | Gravimetric index (%) |
|---|---|---|---|---|
| Hemispherical | 350 bar | Al 6061-O | 1450.97 | 6.31 |
| | | HDPE UHMW | 1403.27 | 6.51 |
| | | Liner-less | 1370.62 | 6.65 |
| | 700 bar | Al 6061-O | 1729.16 | 5.34 |
| | | HDPE UHMW | 1695.66 | 5.45 |
| | | Liner-less | 1667.8 | 5.53 |
| Semi-elliptical | 350 bar | Al 6061-O | 1885.63 | 4.93 |
| | | HDPE UHMW | 1825.66 | 5.08 |
| | | Liner-less | 1780.3 | 5.2 |
| | 700 bar | Al 6061-O | 2323.33 | 4.03 |
| | | HDPE UHMW | 2281.25 | 4.1 |
| | | Liner-less | 2239.29 | 4.18 |

gravimetric indexes of aerogel, polyurethane, and rohacell insulated vessels are 51.4%, 49.1%, and 47.7%, respectively. For the tank capacity of 90.35 kg (orange bars in Figure 8), the gravimetric indexes of the same insulation materials are 52.6%, 50.7%, and 49.5%, respectively. Furthermore, for each insulation solution, the difference in gravimetric index increases as the tank capacity rises, particularly when the thermal performance of the insulation layer is lower. In other words, higher levels of LH/textsubscript[2] stored always result in higher gravimetric indices, and these increases are even greater if traditional insulation, such as Rohacell or Polyurethane, is selected.

The data related to the total storage system weights shown in Figure 9 aligns with that of the gravimetric index in Figure 8 and with the considerations derived above. Indeed, by using four tanks to store the whole amount of fuel required, maximum savings in the total storage system weight have been quantified to 207 kg and 146.75 kg for the two tank capacities corresponding to the PEMFC and SOFC long-term scenarios, respectively. Taking advantage of optimized tank performance, an increase in the aircraft payload or in the mass of hydrogen stored can be foreseen.

It may be worth mentioning that using a single vessel to store all hydrogen required for a mission instead of four equal vessels results in higher maximum gravimetric indexes. For the MLI MD vessel, the indexes are 57.64% and 58.55% for lower and higher storage capacities, corresponding to 281.8 kg and 361.4 kg of $H_2$ (long-term scenarios total-$H_2$ mass requirements in Table 3). As a result, the minimum system weights are 488.87 kg and 617.2 kg, respectively, leading to a reduction of 56.37 kg and 66.48 kg when compared to the best case of the 4-tank configuration, even though the choice of using one single tank may bring with it installation problems and safety issues due to the lack of systems redundancy.

Taking advantage of a case study from the literature, the potential of the parametric model has been demonstrated. The purpose of the study proposed by Marciello et al. is to perform a design exploration considering the whole aircraft system. Instead, the authors propose a deeper analysis to show how the design of the hydrogen storage system can be optimized by taking advantage of a properly designed parametric model. Indeed, it can be easily captured how improvements in the tank gravimetric index greatly impact the system weight, translating into remarkable effects on the entire aircraft design.

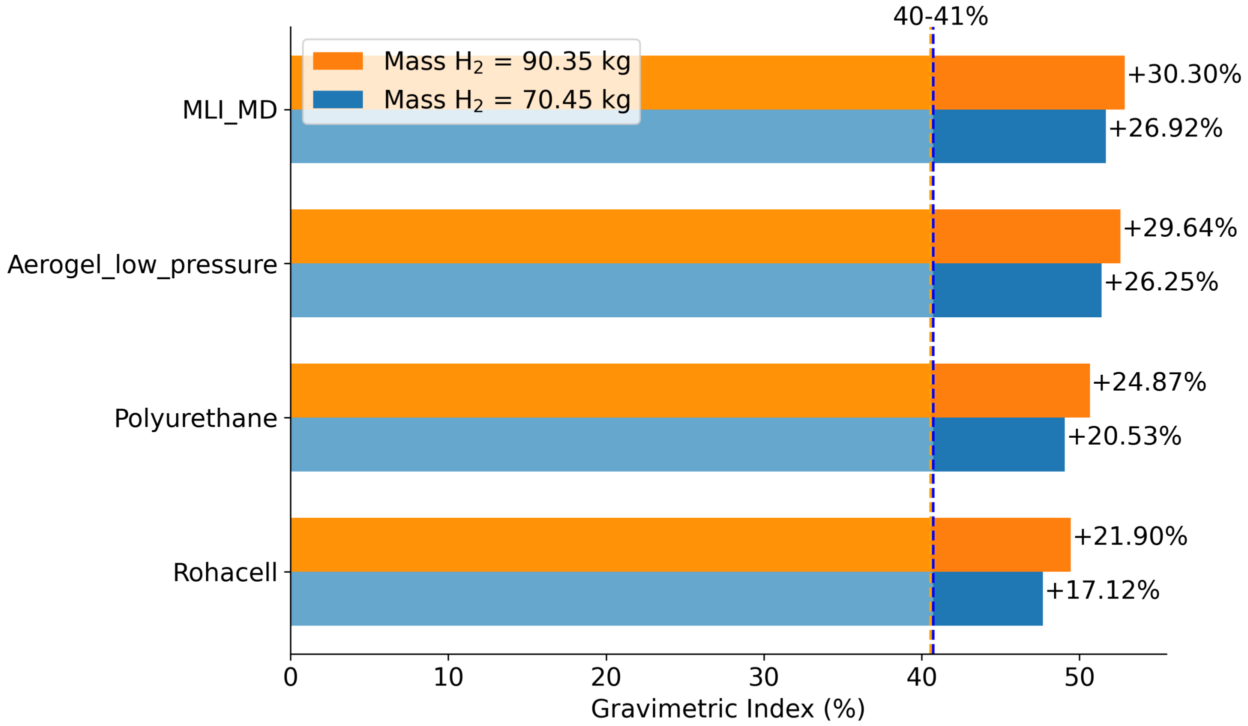


Figure 8 – Percentage increases in the gravimetric index with respect to the ATR reference case (at top of the dashed line) referred to the long-term scenarios (liquid $H_2$ storage) for the two cases of "SOFC + battery" (70.45 kg $H_2$ capacity, in blue) and "PEMFC + battery" (90.35 kg $H_2$ capacity, in orange).

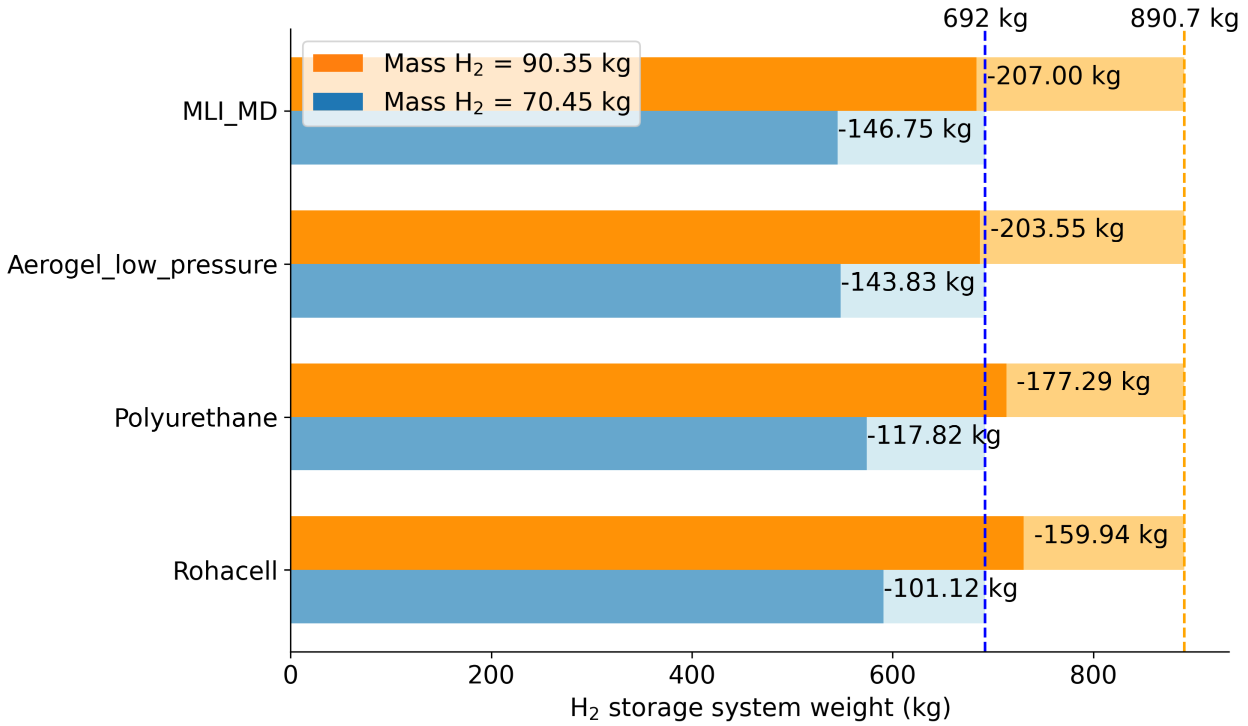


Figure 9 – Total storage system weight decreases with respect to the ATR reference cases (at top of the dashed line) referred to the long-term scenarios (liquid $H_2$ storage) for the two cases of "SOFC + battery" (70.45 kg $H_2$ single tank capacity, in blue) and "PEMFC + battery" (90.35 kg $H_2$ single tank capacity, in orange).

## 5.2 UAV

The second use case selected for the analysis is a small UAV equipped with a $LH_2$ tank built and tested by Adam et al. [26]. The storage vessel has a cylindrical geometry and is wrapped with a vacuum jacket made of aluminum alloy and a thirty-layers MLI. The system is designed and tested for integration with a PEM fuel cell to to improve the UAV endurance. The technical data of interest for the current analysis has been reported in Table 5. The endurance has been estimated only considering the mass flow rate requested by the fuel cell during cruise and the mass of hydrogen stored on-board, assuming the take-off phase to cover a very short segment of the mission profile if compared to its total duration. The details provided in this reference case allowed us to set-up more precisely the model inputs. Indeed, the masses of pipes and supports have been estimated to be 24% of the vessel's weight (considering the inner and outer shell and caps). Then, the model has been set to have the inner and outer aluminum layers, the total weight of such layers has been increased by a 24% correction factor, computed from the masses of the various components provided in the reference, to account for the weight of supports, pipes, and baffle system, and the insulation layer has been allocated in between the two aluminum shells. The mass of hydrogen stored on-board has been calculated from the inner volume of the tank and the ullage, assuming an $LH_2$ density of 70.9 kg/m$^3$. Once the $LH_2$ mass has been found, the gravimetric index has been computed.

Table 5 – Reference data for the UAV use case (elaborated from [26]).

| Property | Value | U.M. |
|---|---|---|
| Ullage | 10 | % |
| Mass flow rate in cruise | 0.0104 | g/s |
| Mass flow rate during take-off | 0.0206 | g/s |
| Pipes and supports weight fraction | 24 | % |
| Total Tank empty weight | 6.3 | kg |
| Gravimetric index | 26.39 | % |
| Inner diameter | 0.52 | m |
| Inner radius | 0.26 | m |
| Inner length | 0.15 | m |
| Max inner volume | 0.032 | m3 |
| Max stored H2 | 2.26 | kg |
| Max endurance | 60.33 | hours |
| Max endurance | 2.51 | days |

The same insulation materials implemented in the previous case study (Sec. 5.1) have been investigated here. The gravimetric indexes resulting from the adoption of rohacell and polyurethane insulation materials are 10.95% and 14.33%, respectively. The tank's empty weights result in 18.37 kg using rohacell material and 15.51 kg with polyurethane insulation. Holding much lower gravimetric indexes than that provided by the literature reference, equal to 24%, their implementation would lead to a dramatic decrease in UAV endurance. Instead, the MLI MD and Aerogel outperform the system presented in the literature. Despite the slight increase in the gravimetric indexes below 2%, relevant improvements in UAV endurance have been identified, as shown in Figure 10. Compared to the literature reference, gravimetric indexes for MLI MD and Aerogel solutions increased by 5.63% and 3.97%, turning into an increase in endurance of 20.05% and 14.34%, respectively.

The results published by Adam et al. [26] come from a more detailed analysis of a vessel that has been built and tested. So, starting from realistic results, a more accurate optimization focusing on the influence of different insulation materials has been proposed here. Unlike what was previously described in the regional aircraft use case, the main performance metric adopted here is flight endurance, which often corresponds to one of the main design goals for UAVs. The optimized vessels hold a gravimetric index that, in both cases, does not exceed by even 2% that retrieved from the literature case. However, dramatic effects on the flight endurance have been highlighted (Figure 10). In addition, it must be mentioned that the study proposed by Adam et al. [26] dates back to 2014. In this

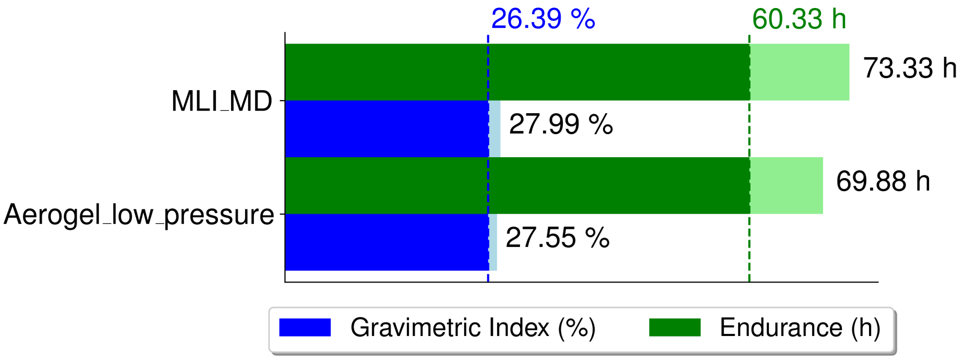


Figure 10 – Gravimetric index and flight endurance comparison with reference case (top of dashed line) for $LH_2$ vessels with Multilayer Mylar/Dacron (MLI MD) and Aerogel at low pressure insulation.

context, considering the innovations introduced in a ten year time interval, the additional value here proposed is a preliminary design update performed thanks to the flexibility of the parametric model introduced in Section 2.

## 6. Conclusions

This study presents a parametric sizing model for designing hydrogen storage vessels. The model follows three subsequent steps: geometric, mechanical, and thermal. The geometric design takes the required inputs, such as the amount of hydrogen mass to be stored, and computes the internal tank geometry. The mechanical design computes the wall thicknesses for composites, metallic, or polymeric materials. Then, the thermal design is performed. If the vessel is requested to store liquid hydrogen at cryogenic conditions, the thermal shield can be sized according to different objectives, such as the maximum admissible boil-off rate or the maximum desired heat power through the tank wall.
Extensive literature research has been conducted to validate the model, and the model outputs have been compared with a series of gravimetric index values. The comparison shows a good agreement between the different data, demonstrating the reliability and effectiveness of the parametric model. The detailed description of the model is covered in the first part of this paper (Sec. 2), and it is followed by its validation (Sec. 3). In Section 4, the compliance between design outputs and future scenarios is checked by collecting technological targets from the main institutional road-maps and agendas. Figure 7 shows that challenging milestones must be achieved, with a gravimetric index of 35% by 2030, and it must be widely exceeded in subsequent years. The research concludes with two case studies from the literature aiming to optimize the performances of $H_2$ storage systems for a regional aircraft and a UAV.

From the preliminary results presented in Sec. 3 and the outputs obtained from the two case studies in Sec. 5, some conclusions can be drawn. The gravimetric index of high-pressure vessels working at ambient temperatures is limited to a range that, in the most realistic scenario, extends up to 15% and does not go above 10% in most cases. On the other hand, the range for liquid $H_2$ tanks is much wider, spanning from around 10% up to more than 70%. The gravimetric efficiencies of $LH_2$ vessels are strongly affected by the amount of fuel to be stored. The curves steeply increase from zero to one hundred kilograms of $H_2$ before moving toward constant values.

The presented case studies highlight how even small improvements leading to gains of a few percentage points in the gravimetric index can translate into significant advantages in terms of weight savings (Sec. 5.1) or flight endurance (Sec. 5.2). The work presented herein demonstrates the flexibility and applicability of the hydrogen storage parametric model and its reliability. It also shows that hydrogen can be a useful alternative to fossil fuels both from the point of view of polluting emissions and performances. Efforts and investments in research can lead to relevant technological advances that will accomplish future targets towards net-zero emissions.

## 7. Contact Author Email Address

mailto: filippo.mazzoni@polito.it

## 8. Copyright Statement



## References

[1] Programme overview and structure | Clean Aviation.

[2] Ahmad Baroutaji, Tabbi Wilberforce, Mohamad Ramadan, and Abdul Ghani Olabi. Comprehensive investigation on hydrogen and fuel cell technology in the aviation and aerospace sectors. 106:31–40.

[3] Gdaniel Brewer. *Hydrogen Aircraft Technology*. Routledge, 1 edition.

[4] S. Sarkar, G. Grandi, and S. Patel. Hydrogen Fuel System for Aircraft. In *SAE Technical Papers*.

[5] K. Swider-Lyons, R. Stroman, J. Rodgers, D. Edwards, J. Mackrell, M. Schuette, and G. Page. Liquid hydrogen fuel system for small unmanned air vehicles. In *51st AIAA Aerospace Sciences Meeting Including the New Horizons Forum and Aerospace Exposition 2013*.

[6] P. Rompokos, A. Rolt, A. Rolt, T. Sibilli, and C. Benson. Cryogenic fuel storage modelling and optimisation for aircraft applications. In *Proceedings of the ASME Turbo Expo*, volume 6.

[7] D. Verstraete, P. Hendrick, P. Pilidis, and K. Ramsden. Hydrogen fuel tanks for subsonic transport aircraft. 35(20):11085–11098.

[8] Linus Kameni Monkam, Arne Graf von Schweinitz, Jens Friedrichs, and Xin Gao. Feasibility analysis of a new thermal insulation concept of cryogenic fuel tanks for hydrogen fuel cell powered commercial aircraft. 47(73):31395–31408.

[9] Chana Anna Saias, Ioannis Roumeliotis, Ioannis Goulos, Vassilios Pachidis, and Marko Bacic. Assessment of hydrogen fuel for rotorcraft applications. 47(76):32655–32668.

[10] David Cohen, Susan C Mantell, and Liyang Zhao. The effect of fiber volume fraction on filament wound composite pressure vessel strength. 32(5):413–429.

[11] Eugenio G. M. Brusa and Matteo Nobile. *Assessment of a Design Method for Composite Over-Wrapped Pressure Vessels for Hydrogen Storage*, volume Volume 1: Advanced Energy Systems, Advanced Materials, Aerospace, Automation and Robotics, Noise Control and Acoustics, and Systems Engineering of *Engineering Systems Design and Analysis*.

[12] Nicholas A. Klymyshyn, Kriston Brooks, and Nathan Barrett. Methods for Estimating Hydrogen Fuel Tank Characteristics. 146(011501).

[13] Yunus A. Çengel, Michael A. Boles, and Kanoğlu Mehmet. *Thermodynamics: An Engineering Approach / Yunus A. Çengel, Michael A. Boles, Mehmet Kanoğlu*. McGraw-Hill, 9th ed edition.

[14] Dries Verstraete. The Potential of Liquid Hydrogen for long range aircraft propulsion.

[15] Saurav Tiwari, Michael J. Pekris, and John J. Doherty. A review of liquid hydrogen aircraft and propulsion technologies. 57:1174–1196.

[16] Afshin Ghajar and Yunus Cengel. *Heat and Mass Transfer - Fundamentals and Applications, 6th Edition, McGraw-Hill Education, New York, NY, 2020.*

[17] Maria Chiara Massaro, Roberta Biga, Artem Kolisnichenko, Paolo Marocco, Alessandro Hugo Antonio Monteverde, and Massimo Santarelli. Potential and technical challenges of on-board hydrogen storage technologies coupled with fuel cell systems for aircraft electrification. 555:232397.

[18] Eytan J. Adler and Joaquim R. R. A. Martins. Hydrogen-powered aircraft: Fundamental concepts, key technologies, and environmental impacts. 141:100922.

[19] Net Zero Roadmaps.

[20] Programme overview and structure | Clean Aviation.

[21] Concepts.

[22] ZEROe - Low carbon aviation - Airbus.

[23] Key documents | Clean Aviation.

[24] FlyZero Reports Archive.

[25] Valerio Marciello, Mario Di Stasio, Manuela Ruocco, Vittorio Trifari, Fabrizio Nicolosi, Markus Meindl, Bruno Lemoine, and Priscilla Caliandro. Design Exploration for Sustainable Regional Hybrid-Electric Aircraft: A Study Based on Technology Forecasts. 10(2):165.

[26] P. Adam and J. Leachman. Design of a reconfigurable liquid hydrogen fuel tank for use in the genii unmanned aerial vehicle. volume 1573, pages 1299–1304.